

## Supporting information

### **Large-area 2D Bismuth Antimonide with Enhanced Thermoelectric Property via Multiscale Electron-Phonon Decoupling**

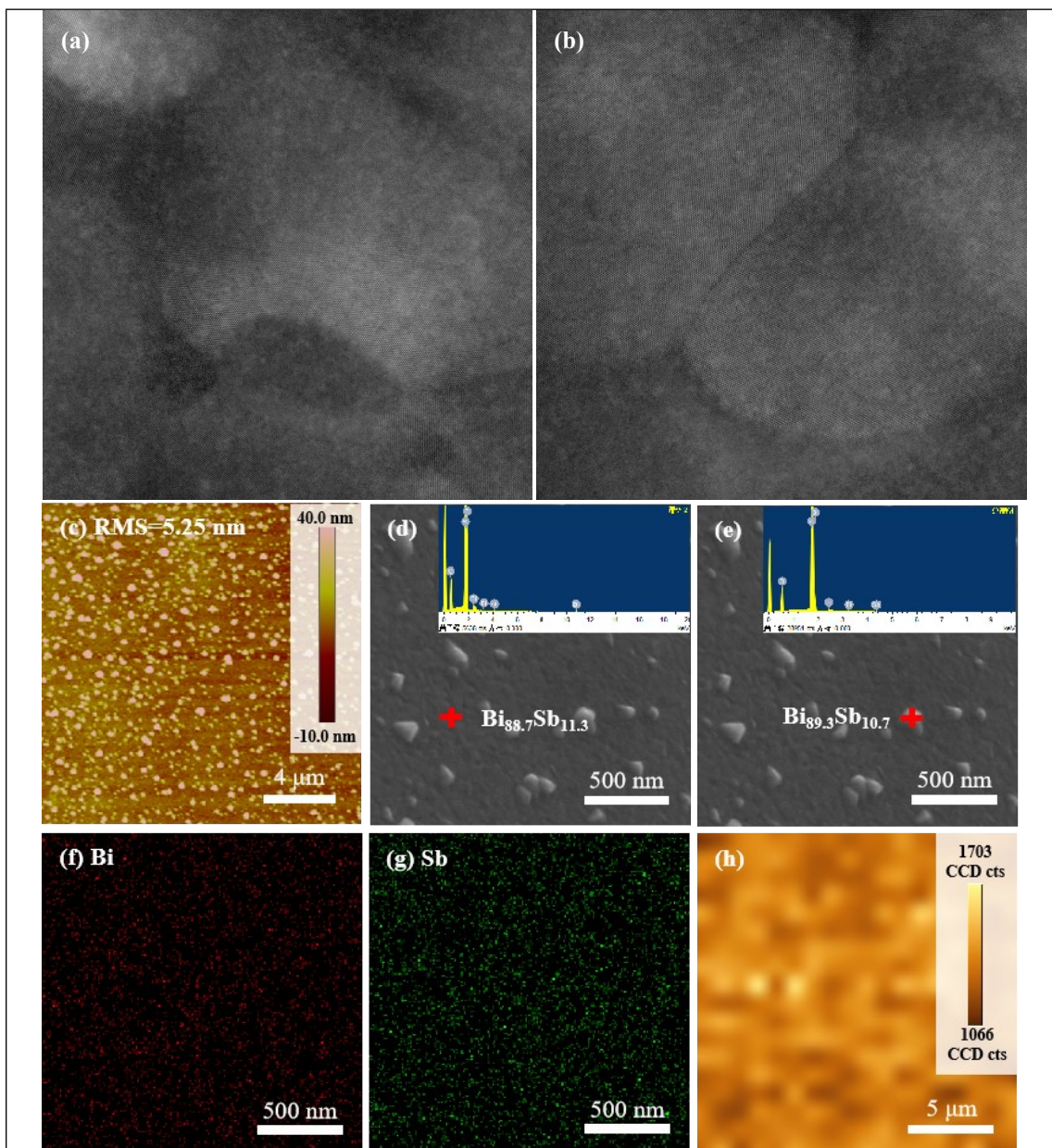
Hanliu Zhao<sup>a‡</sup>, Yuxin Xue<sup>a‡</sup>, Yu Zhao<sup>b‡</sup>, Jiayi Chen<sup>a</sup>, Bo Chang<sup>a</sup>, Hao Huang<sup>a</sup>, Tao Xu<sup>c</sup>, Litao Sun<sup>c</sup>, Yunfei Chen<sup>b</sup>, Jingjie Sha<sup>b,\*</sup>, Beibei Zhu<sup>a,\*</sup>, Li Tao<sup>a,\*</sup>

<sup>a</sup> School of Materials Science and Engineering, Jiangsu Key Laboratory of Advanced Metallic Materials, Southeast University, Nanjing 211189, People's Republic of China

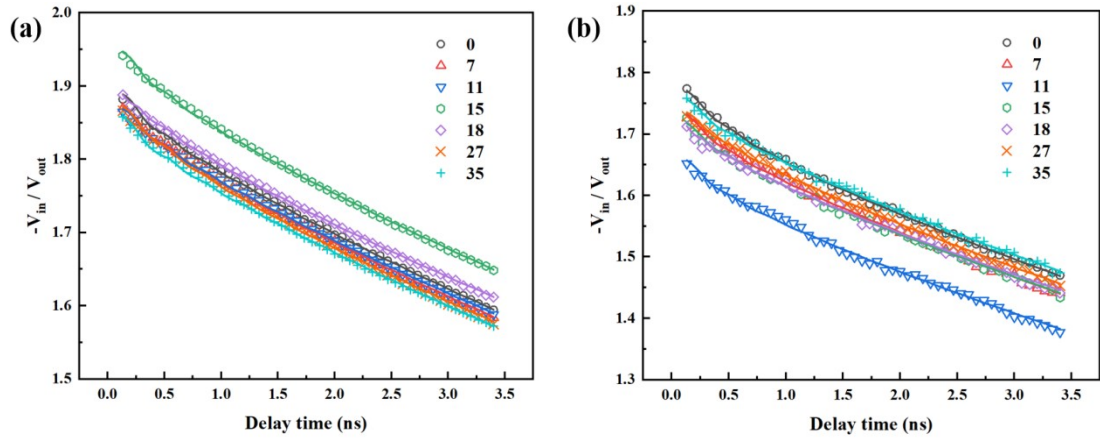
<sup>b</sup> School of Mechanical Engineering, Jiangsu Key Laboratory for Design and Manufacture of Micro-Nano Biomedical Instruments, Southeast University, Nanjing 211189, People's Republic of China

<sup>c</sup> SEU-FEI Nano-Pico Center, Key Laboratory of MEMS of Ministry of Education, Collaborative Innovation Center for Micro/Nano Fabrication, Device and System, Southeast University, Nanjing 211189, People's Republic of China

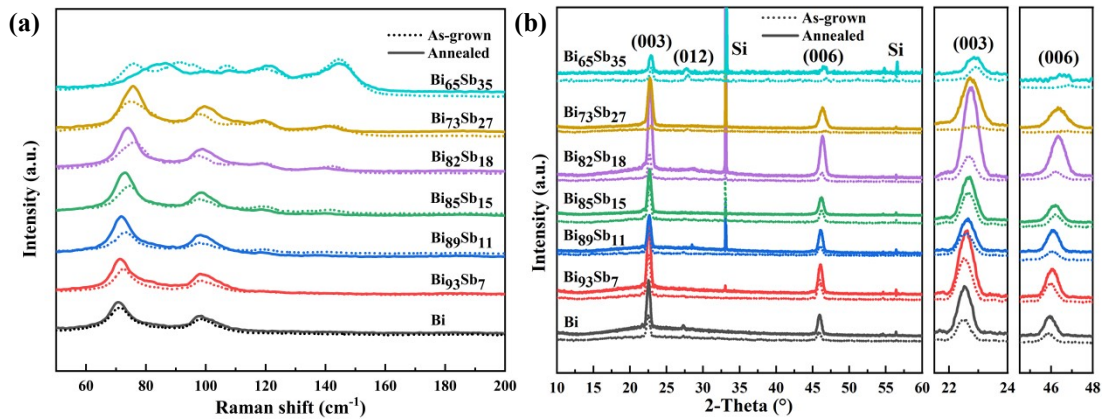
E-mail: tao@seu.edu.cn, 101012333@seu.edu.cn, major212@seu.edu.cn



**Fig. S1 (a&b) TEM images of 2D  $\text{Bi}_{82}\text{Sb}_{18}$ . (c) AFM image of 2D  $\text{Bi}_{82}\text{Sb}_{18}$ , showing a roughness of 5.25 nm. (d&e) Point EDS results of flat area and the protruded grains in  $\text{Bi}_{89}\text{Sb}_{11}$ . (f&g) EDS mapping of 2D  $\text{Bi}_{65}\text{Sb}_{35}$ . (h) Raman mapping of 2D  $\text{Bi}_{82}\text{Sb}_{18}$ .**

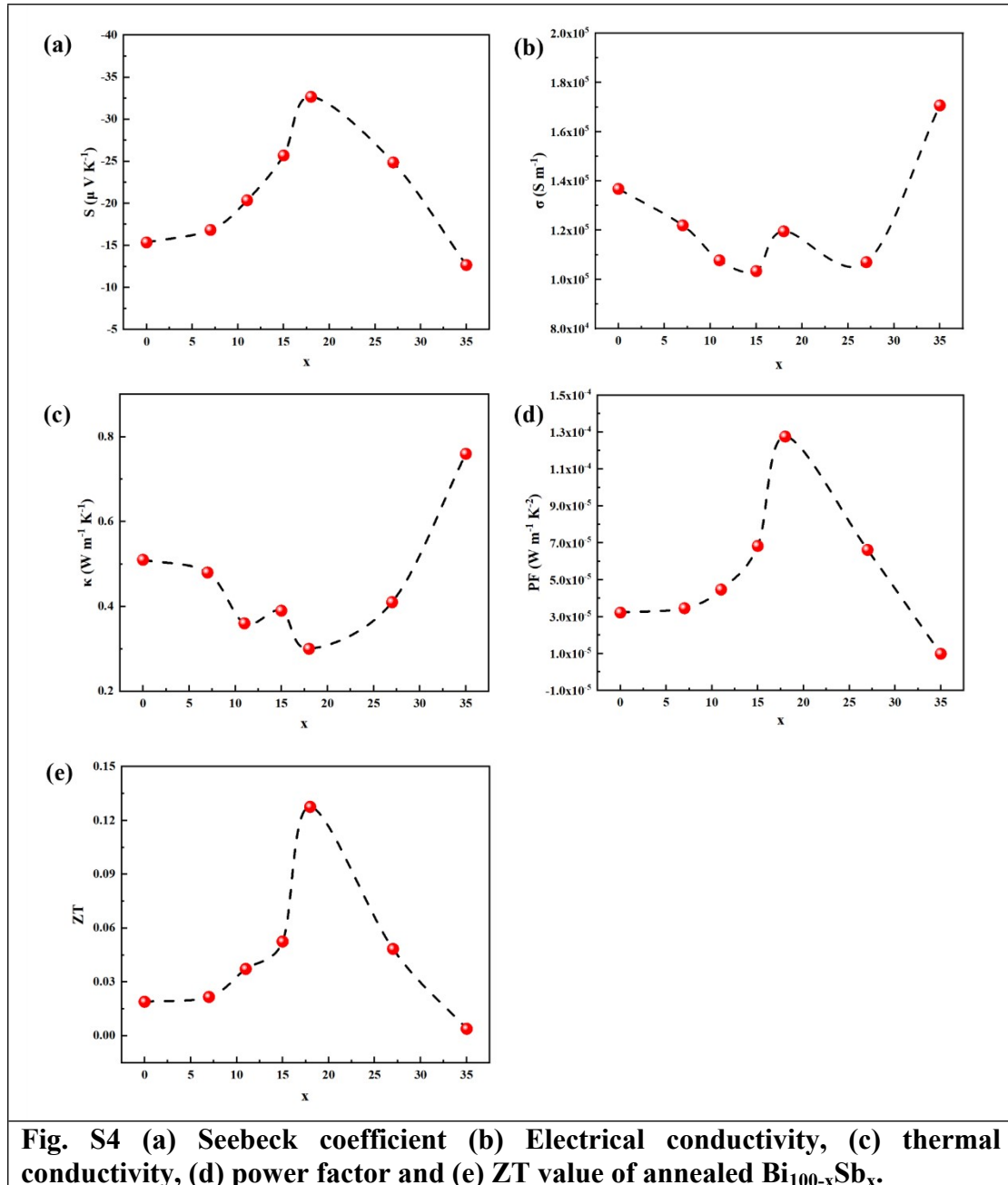


**Fig. S2** Fitting curves of  $-V_{in}/V_{out}$ -delay time for TDTR measurement of (a) as-grown and (b) annealed 2D bismuth antimonide.  $V_{in}$  and  $V_{out}$  represent in-phase and out-of-phase signals, respectively. The open symbols and the solid lines denote measured data and thermal model fitting result. Measurement conditions: modulation frequency: 1.72 MHz; pump beam spot size: 10  $\mu\text{m}$ ; probe spot size: 6.0  $\mu\text{m}$ .



**Fig. S3** (a) XRD patterns and (b) Raman spectra of as-grown and annealed 2D bismuth antimonide

After annealing process, the absolute Seebeck coefficient values are increased when  $x=15, 27$  and  $35$  but decreased when  $x=0, 7$  and  $11$  (Fig. S4a). There may be two reasons: i) the sublimation in the samples with  $x=0, 7$  and  $11$  is negligible in SEM image (Fig. S7); ii) the annealing treatment reduces the density of defects. The above situations will reduce the electron scattering and cause the Seebeck coefficient decreasing.



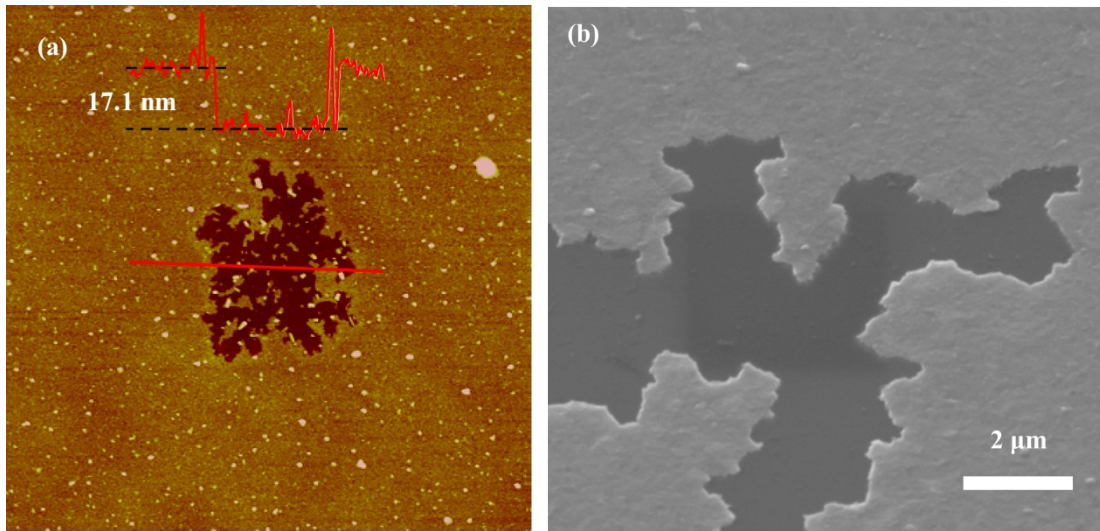


**Fig. S5 AFM and SEM images of annealed 2D  $\text{Bi}_{82}\text{Sb}_{18}$ .**

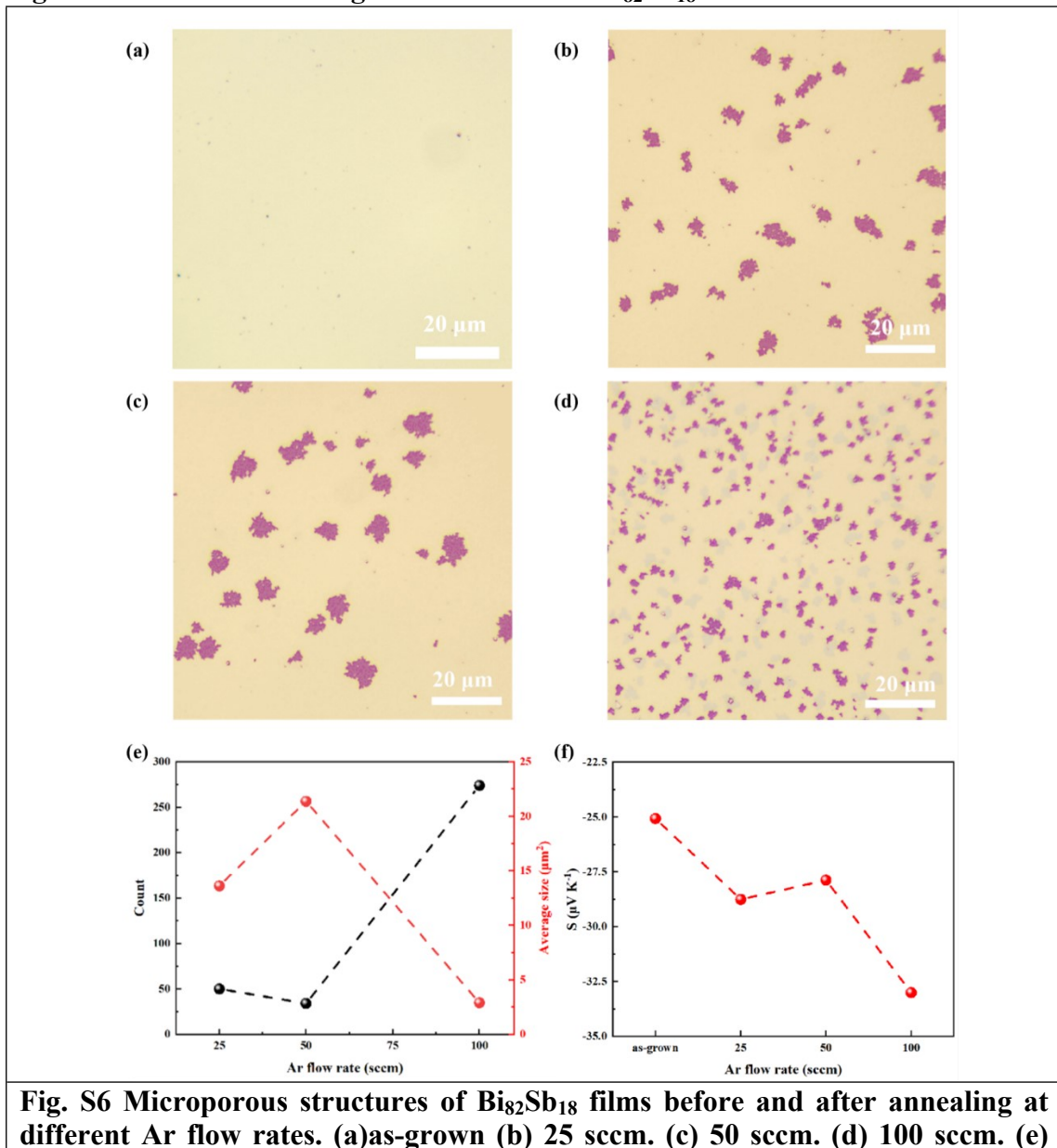


**Fig. S6 Microporous structures of  $\text{Bi}_{82}\text{Sb}_{18}$  films before and after annealing at different Ar flow rates. (a) as-grown (b) 25 sccm. (c) 50 sccm. (d) 100 sccm. (e)**

number of micropores and average size. (f) Seebeck coefficient.

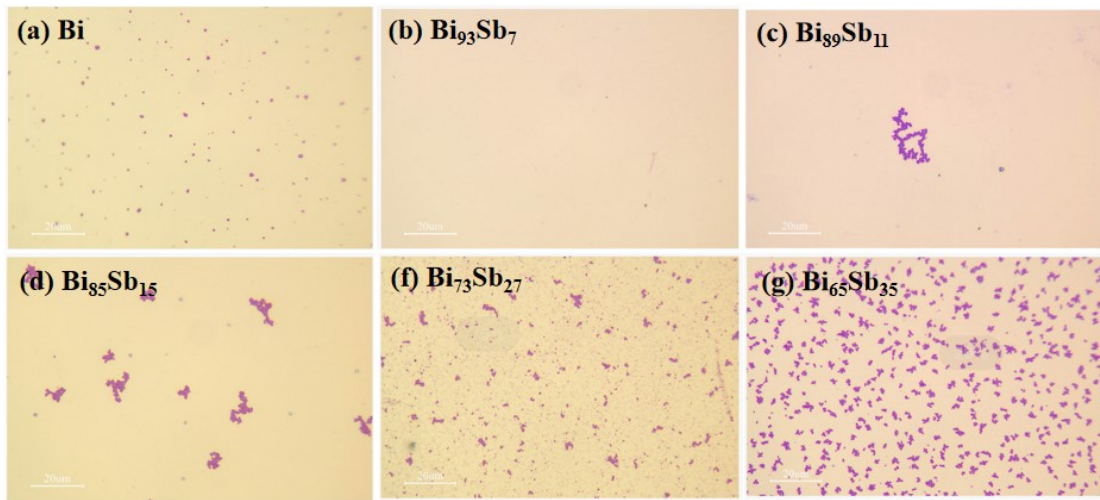


Fig. S7 OM images of annealed 2D Bi<sub>1-x</sub>Sb<sub>x</sub>.